Sensorless Kinesthetic Teaching of Robotic Manipulators Assisted by Observer-Based Force Control

Capurso, Martino; Ghazaei, Mahdi; Johansson, Rolf; Robertsson, Anders; Rocco, Paolo

Published in:
Proceedings of IEEE International Conference on Robotics and Automation (ICRA) 2017

DOI:
10.1109/ICRA.2017.7989115

2017

Sensorless Kinesthetic Teaching of Robotic Manipulators Assisted by Observer-based Force Control

Martino Capurso[1], M. Mahdi Ghazaei Ardakani[2], Rolf Johansson[2], Anders Robertsson[2], Paolo Rocco[1]

***Abstract*— In modern day industry, robots are indispensable for achieving high production rates and competitiveness. In small and medium scale enterprises, where the production may shift rapidly, it is vital to be able to reprogram robots quickly. Kinesthetic teaching, also known as lead-through programming (LTP), provides a fast approach for teaching a trajectory. In this approach, a trajectory is demonstrated by physical interaction with the robot, i.e., the user manually guides the manipulator. This paper presents a sensorless approach to LTP for redundant robots that eliminates the need for expensive force/torque sensors. The active implementation enhances the passive LTP by an admittance control in joint space based on the external forces applied by the user, estimated with a Kalman filter using the generalized momentum formulation. To improve the quality of the estimation and hence LTP, we use a dithering technique. The active LTP has been implemented on ABB YuMi robot and experimental comparison with an earlier passive LTP is presented.**

I. Introduction

Nowadays, a high level of automation in manufacturing plants is essential to guarantee competitiveness in the market. Apart from the complexity of the tasks, the programming phase is one of the main obstacles to the wide employment of robots in small-series productions or production lines that have to be frequently reconfigured. Often, to program the tasks that a robot has to accomplish, a teach pendant and/or 3D software are utilized. These methods are generally time consuming, which implies an increase of the production cost.

An alternative approach is through direct interaction with the robot, which is called kinesthetic teaching or lead-through programming (LTP). The aim is to demonstrate a movement to a robot, i.e., an operator moves the robot while the trajectory data are being recorded. Evidently, the robot can not be moved if it has been made stiff by the position feedback. A solution is to adjust the feedback based on sensing of external forces. To detect the external forces, force/torque sensors can be employed. However, the sensors can be fragile and costly in addition to reducing the maximum payload of a robot. This is especially the case when a redundant robot is used and it is desired to measure forces exerted on any part of the robot, and not only the end effector.

[1]M. Capurso and P. Rocco are with Politecnico di Milano, Dipartimento di Elettronica, Informazione e Bioingegneria, Piazza L. Da Vinci 32, 20133 Milano, Italy.

[2] M. M. Ghazaei Ardakani, R. Johansson and A. Robertsson are with the Department of Automatic Control, LTH, Lund University, SE–221 00 Lund, Sweden. The authors are members of the LCCC Linnaeus Center and the eLLIIT Excellence Center at Lund University. The corresponding author is M. M. Ghazaei A., E–mail: mahdi.ghazaei@control.lth.se

For these reasons, various sensorless schemes have been suggested relying on force estimation techniques. In general, there are two main approaches for estimating external forces: using a disturbance observer based on the control error, or a force observer utilizing in addition the knowledge of motor torques. Disturbance observers based on joint angle measurements have been analyzed in [1], [2]. The idea of force observer for collision detection based on the generalized momentum has been introduced in [3]. The generalized momentum formula is particularly convenient since it does not require the numerical differentiation of velocity as used in [4] nor the inversion of the inertia matrix. In [5], a recursive least-squares estimation of force as well as an observer-based method based on the generalized momentum formulation have been discussed and compared. The force observer approach has further been extended to estimate the end-effector forces directly in the Cartesian space [6].

Force sensing together with force control can make up an LTP system. As an example, [7] describes an active LTP, where the aim is to improve the programming accuracy using force control, with a sensorless approach, on one operational space degree of freedom at a time; several limits and constraints have been applied to ensure safety during human-robot interaction. In general, the interplay between the force estimation and force control may cause instabilities in stiff contact situations. Therefore, to allow a stable interaction with highly stiff materials, a passive approach (no feedback of interaction force) has been proposed [8]. In this method, the robot is gravity and partially friction compensated. Using high values for the integral gain in the internal PID controllers has been suggested for reducing the effect of stiction before the start of motion.

Although the passive approach solves the instability issues, the overall performance is limited by the intrinsic mechanical properties of the robot. On the other hand, when force feedback is used, the physical properties of the closed loop system such as inertia and damping can be altered. The force feedback can be utilized to shape the behavior of the robot in several ways such as introducing motion constraints. Therefore, it is worthwhile to investigate if these two approaches can be combined.

This paper presents a sensorless active LTP which builds on the passive approach introduced in [8] by adding a force estimation block and an admittance control architecture. The external forces are estimated using a Kalman filter in joint space based on the generalized momentum formulation. Following the ideas of [9], a dithering signal is added to the non-rotating joints to reduce the effect of the static friction

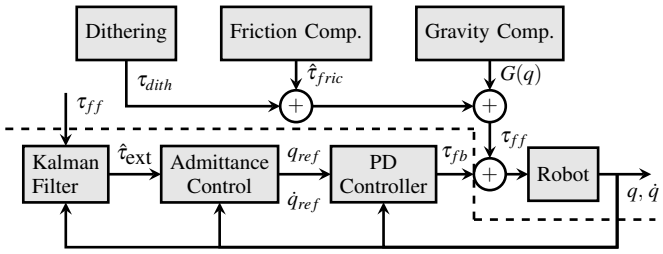

Fig. 1. Control scheme: the estimated external torque is the input of the admittance control, which generates the references for the PD controller. The resulting motor torque is then added to the feedforward component that is the superposition of gravity and friction compensation and dithering torques. The components specific to the active LTP approach lie below the dashed line.

and to improve the detection of forces.

The rest of the article is organized as follows. Section II presents the methods, in which the disturbance observer and the admittance control architecture are described. In Sec. III, the experimental results of the observer as well as the active LTP are illustrated, with particular attention to the dithering method. A comparison between our active LTP and a previously implemented passive LTP is also presented. We discuss the results in Sec. IV and draw conclusions in Sec. V.

II. Methods

In this section, we discuss different methods required to implement our active LTP system. The system presented in this paper extends a passive LTP, realized by compensating the gravity load and part of the friction present in the joints. The gravity load on each joint can be calculated once a dynamic model of the robot is available, then the compensation torque can be applied in feedforward. The force control based on the estimated force runs in parallel with the passive LTP as shown in the overall block diagram of the system in Fig. 1.

Firstly, the control structure of the active LTP based on the admittance control is presented. This is followed by the description of an experimental friction model and our friction compensation method. Subsequently, the details of the force observer based on the generalized momentum formulation is given. Finally, we describe the dithering method that improves the passive as well as the active LTP.

A. Controller

In this section, the force control architecture using the estimated external torques is described. As for the force feedback, we use an *admittance control*, which receives the estimated torques in each joint as inputs and calculates the desired joint velocities [10].

The equations of motion of a manipulator with n degrees of freedom can be written as

$$M(q)\ddot{q} + C(q,\dot{q})\dot{q} + G(q) + \tau_{fric}(\dot{q},q) + \tau_{ext} = \tau, \quad (1)$$

where $q \in \mathbb{R}^n$ denotes the joint angles, $\tau_{ext} \in \mathbb{R}^n$ are the external torques on joints, $M \in \mathbb{R}^{n\times n}$ denotes the inertia matrix, $C \in \mathbb{R}^{n\times n}$ the Coriolis matrix, $G \in \mathbb{R}^{n\times n}$ the gravity load, $\tau_{fric} \in \mathbb{R}^n$ the friction torque and $\tau \in \mathbb{R}^n$ the motor torque on the arm side.

In the active implementation, the motor torque is calculated as the superposition of the feedforward component and the feedback component

$$\tau = \tau_{ff} + \tau_{fb}, \quad (2)$$

$$\tau_{ff} = G(q) + \varepsilon\hat{\tau}_{fric}(q,\dot{q}) + \tau_{dith}, \quad (3)$$

$$\tau_{fb} = K_P(q_{ref} - q) + K_D(\dot{q}_{ref} - \dot{q}). \quad (4)$$

The feedforward component is denoted by τ_{ff}; the term ε is an empirical coefficient for a percentage of the modeled friction to be compensated and τ_{dith} denotes the dithering torque. The feedback component τ_{fb} is the output of a PD controller. No integral part is employed since the exact tracking of the reference is not important in the basic application of LTP. The position and velocity references are generated by the admittance control algorithm

$$\ddot{q}_{ref} = \tilde{M}(q)^{-1}(\hat{\tau}_{ext} - \tilde{D}\dot{q}), \quad (5)$$

where $\hat{\tau}_{ext}$ is the estimated torque, and the matrices $\tilde{M}$ and $\tilde{D}$ represent the desired inertia and damping matrices, respectively. These matrices define the desired behavior of the manipulator and can be tuned. For instance, if the arm is expected to react as a heavily damped system, a higher value for the $\tilde{D}$ matrix is chosen. In our experiments, we have set $\tilde{M}$ proportional to $M(q)$ in (1) and chosen a diagonal matrix $\tilde{D}$. The position and velocity references can be obtained from numerical integration of $\ddot{q}_{ref}$.

B. Friction Compensation

The friction model plays a two-fold role in our system. It is essential for a good estimate of external torques by the observer as well as it is used to compensate a portion of the friction torque with a feedforward torque signal.

We regard the friction torque as a known disturbance that has to be properly modeled. In order to define the friction model parameters and the friction torque, experimental tests were carried out on each joint. Similar to the experiments presented in [11], each joint was moved back and forth with a square-wave acceleration profile. The outcome of the test is a velocity-motor torque curve, which after filtering and gravity compensation, shows a trend due to Coulomb and viscous friction. As explained in [11], the S-shaped trend of the friction torque can be well captured by two sigmoid functions, defined as

$$\tau_{f,max}(\dot{q}) = \tau_{C,min} + \frac{\tau_{C,max} - \tau_{C,min}}{1 + e^{-A(\dot{q}+B)}} + c\dot{q}, \quad (6)$$

$$\tau_{f,min}(\dot{q}) = \tau_{C,min} + \frac{\tau_{C,max} - \tau_{C,min}}{1 + e^{-A(\dot{q}-B)}} + c\dot{q}, \quad (7)$$

where τ_C is the Coulomb friction, the parameter A describes the slope of the sigmoid function, the parameter B is the width of the area between the curves and finally there is a linear term $c\dot{q}$ to model the viscous component.

Once these parameters are identified, a probabilistic friction model can be obtained as a velocity-dependent random variable with the mean value equal to the average of these

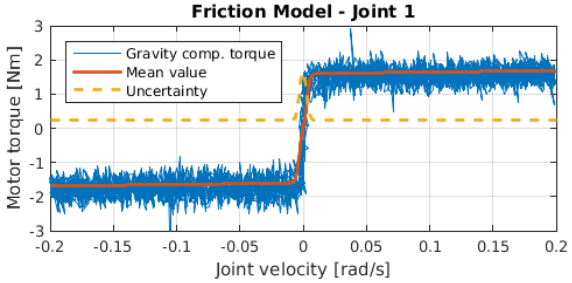

Fig. 2. Friction model: the blue curves correspond to the measured data after gravity compensation. The typical trend due to Coulomb and viscous friction can be noticed. The model consists of a velocity-dependent Gaussian random variable. The mean value (red line) and the corresponding standard deviation (dashed line) are illustrated.

bounds. The mean value of the total friction (due to Coulomb and viscous components) and the uncertainty as a function of velocity are depicted in Fig. 2. In particular, it can be noticed that the friction is equal to zero with a large uncertainty in a small range at almost zero velocity. This is due to the fact that when the joint is not moving, the magnitude of the friction can take any value between the minimum and the maximum of the Coulomb component.

The friction compensation torque has been calculated similarly to [8], based on the friction model presented in Sec. II-B. The friction is compensated at non-zero velocities, i.e., as soon as the joint starts rotating. Ideally, it is desired to compensate friction completely, then the arm would be free-floating with no drifts. In practice, because of uncertainties and disturbances, only 80% of the modeled friction was compensated by setting $\varepsilon = 0.8$.

C. Kalman Filter Based on the Generalized Momentum

Existing force estimation schemes relying on the robot dynamics typically involve computation of joint accelerations or inversion of the inertia matrix. The former approach requires numerical differentiation of joint speeds resulting in the amplification of measurement noise, while the latter may be computationally costly and prone to numerical issues. A force observer in joint space based on the generalized momentum approach, as opposed to the previous formulations, does not require the numerical acceleration nor the inversion of the inertia matrix [6].

Recalling the equation of motion of the robot (1), the generalized momentum is given by

$$p = M(q)\dot{q}, \tag{8}$$

and the differentiation with respect to time results in

$$\dot{p} = \dot{M}(q)\dot{q} + M(q)\ddot{q}. \tag{9}$$

Substituting (9) into (1) results in

$$\dot{p} = \dot{M}(q)\dot{q} + \tau - C(q,\dot{q})\dot{q} - G(q) - \tau_{fric}(\dot{q},q) - \tau_{ext}. \tag{10}$$

Assuming that the Coriolis matrix is expressed using Christoffel symbols [12], $(\dot{M} - 2C)$ is a skew-symmetric matrix and with the symmetry of M, we conclude

$$\dot{M} = C + C^T.$$

Accordingly, (10) can be further simplified to

$$\dot{p} = C(q,\dot{q})^T\dot{q} - G(q) + \tau - \tau_{fric}(\dot{q},q) - \tau_{ext}. \tag{11}$$

The key idea is to combine the description of the manipulator dynamics based on the generalized momentum with well-known disturbance observer approaches [6]. To this purpose, the external torques can be modeled as

$$\dot{\tau}_{ext} = A_\tau \tau_{ext} + w_\tau, \tag{12}$$

where w_τ is the Gaussian white noise (or uncertainty), with intensity Q_τ; the subscript τ indicates that it is related to the external torque. Unless a model of external forces are available, we assume constant torques at the joints by setting $A_\tau = 0$.

A joint friction estimate $\hat{\tau}_{fric}$ is assumed to be available, where uncertainties in friction estimates are modelled as white noise w_p with intensity of Q_p

$$w_p = \hat{\tau}_{fric} - \tau_{fric}. \tag{13}$$

The subscript p stands for process, since friction is the major source of uncertainties in the model. The term $\hat{\tau}_{fric}$ and the white noise w_p are determined using the friction model defined in Section II-B. Note that the friction model assumes a velocity-dependent mean and uncertainty.

Substituting (13) into (11), the generalized momentum dynamics can be expressed as

$$\dot{p} = u - \tau_{ext} + w_p, \tag{14}$$

where the term u is defined as

$$u := \tau + C(q,\dot{q})^T\dot{q} - G(q) - \hat{\tau}_{fric}(\dot{q},q). \tag{15}$$

The above equation can be reformulated in the state-space form by augmenting the states with the external forces according to (12) and adding a measurment equation

$$\begin{aligned} \overbrace{\begin{bmatrix}\dot{p}\\ \dot{\tau}_{ext}\end{bmatrix}}^{\dot{x}} &= \overbrace{\begin{bmatrix}0_n & -I_n\\ 0_n & A_\tau\end{bmatrix}}^{A}\overbrace{\begin{bmatrix}p\\ \tau_{ext}\end{bmatrix}}^{x} + \overbrace{\begin{bmatrix}I_n\\ 0_n\end{bmatrix}}^{B}u + \overbrace{\begin{bmatrix}w_p\\ w_\tau\end{bmatrix}}^{w},\\ y &= \underbrace{\begin{bmatrix}I_n & 0_n\end{bmatrix}}_{C}\begin{bmatrix}p\\ \tau_{ext}\end{bmatrix} + v \end{aligned} \tag{16}$$

where u is considered as the input and v is the measurement noise with intensity R.

The observer corresponding to system (16) is

$$\begin{cases}\dot{\hat{x}} = A\hat{x} + Bu + K(y - \hat{y})\\ \hat{y} = C\hat{x}\end{cases} \tag{17}$$

where K is the Kalman gain matrix calculated as

$$K = PC^TR^{-1} \tag{18}$$

and P is the error covariance matrix. The matrix P is in general time-varying and is obtained by solving the differential Riccati equation [13]. However, as shown in Fig. 2, the velocity-dependent uncertainty in the friction can be approximated by two levels: a constant high value for low velocities and a lower value for velocities higher than a

defined threshold. Since the system matrices are constant and noise intensities are not changing over a large range, two constant values for the gain of Kalman filters K can be defined for each joint, approximating the solution with stationary values. Accordingly, we solve the algebraic Riccati equation (ARE)

$$AP + PA^T - PC^T R^{-1} CP + Q = 0, \tag{19}$$

where the matrix Q denotes the intensity of the state noise

$$Q = \text{blockdiag}([Q_p, Q_\tau]).$$

The Kalman gains are calculated off-line and then recalled during the real-time execution. Finally, the estimate of external torques on joints can be obtained from the estimated state $\hat{x}$.

D. Dithering

As can be seen in (17), the inputs of the observer are the artificial torque u, defined in (15), and the measured generalized momentum y. It is clear that, if the measured joint velocity is null both y and $\hat{\tau}_{fric}$ are zero. This implies that the estimated torque depends incorrectly on the sum of the external torque and the static friction (which can be zero). Therefore, the Kalman filter based on the generalized momentum can only estimate correctly the forces that overcome the static friction.

An effective strategy to reduce the required forces to overcome the static friction and produce rotation of the joint is using a *dithering torque* [9]. A torque signal at high frequency with a square wave shape is added to the feedforward torque when the joint is not moving. The amplitude of the dithering torque is small enough not to make the joint move, but at the same time the resulting vibrating effect averages out the static friction in the harmonic gear box of the joint improving the estimation quality. The dithering torque is then deactivated as soon as the joint starts rotating.

III. Experimental Results

All the experiments were done using ABB YuMi robot, a dual-arm manipulator, with 7 joints for each arm [14]. The robot is designed to operate in a work environment shared with humans. For this reason, it has power and speed limitations and soft padding to cover all sharp edges. For the implementation of the methods in Sec. II, we made use of the external research interface described in [15], that allows to interact with and modify the native controller of the robot.

An ATI Mini40 force/torque sensor [16] was mounted on the flange, which was only used for the validation phase. The raw measurements in the sensor frame were converted to the end-effector frame, scaled with the sensitivity of the sensor, and compensated for the gravity component. The corresponding torques on joints were calculated as

$$\tau_{ext} = J^T F_{ext}, \tag{20}$$

where $F_{ext} \in \mathbb{R}^6$ is the vector of wrenches, i.e., the forces and torques at the end-effector frame and J is the geometrical Jacobian with respect to the end-effector.

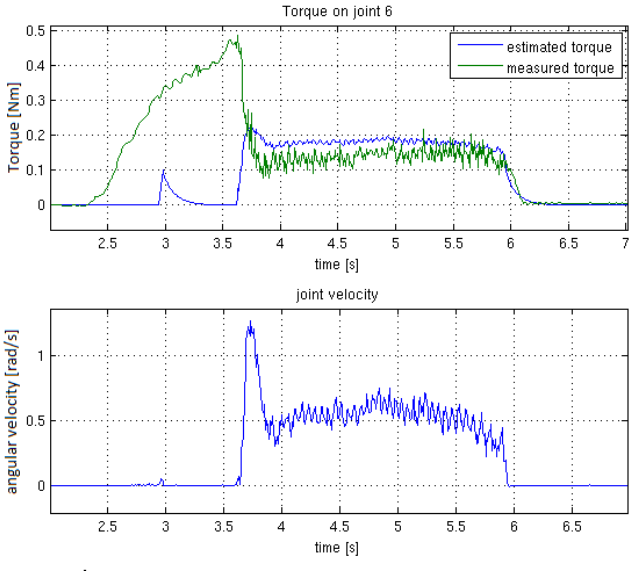

Fig. 3. Measured and estimated torques on joint six. When the joint is not moving, the observer cannot estimate the external torque. After the movement of the joint, the estimate converges to the measured value.

In the next sections, the experiments are described. Firstly, we present the results related to the estimation of external forces. The importance of the dithering torque at zero-velocity has been illustrated. Secondly, we present an example illustrating the functionality of the active LTP proposed in this article, and finally a comparison between our active LTP and a passive LTP [8] is presented.

A. Force Observer

Here, we present the result of the force estimation method described in Sec. II-C. The wrist-mounted force sensor was used to verify the results after tuning the observer. In the first experiment, the feedforward compensation of gravity and friction was activated. Figure 3 shows the result of the estimation. The estimation error can be attributed to the transients of the filters and inaccurate model parameters. Most importantly, the external force has to overcome the static friction before being detected by the Kalman filter. Therefore, in the next experiment we applied a feedforward dithering torque. A square-wave dithering signal was chosen with a frequency of 15 Hz and an amplitude equal to 20% of the modeled friction. The relation between the frequency and the noise in the measured velocity was evaluated while ensuring the high responsiveness of the system.

Figure 4 compares the result of moving a joint of the robot firstly without the dithering torque at almost-zero velocities and secondly when the dithering was active. It was noticed that the required torque to overcome the static friction is almost half of the one without dithering, leading to a smaller step in the velocity and lower latency between the application of the external torque and its detection. The dithering torque was automatically deactivated as soon as the joint started rotating.

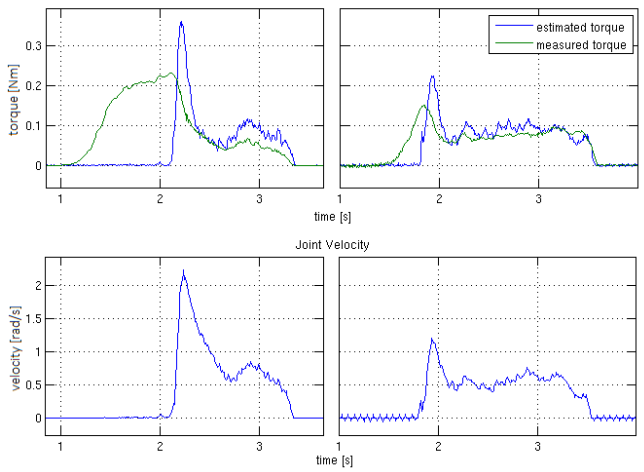

Fig. 4. The effect of dithering: the joint is moved firstly without the dithering torque at zero velocity (on the left), secondly after it has been activated (on the right). The measured initial torque required to start moving the joint is almost half of the first case. The slight oscillation in the velocity is because of the large amplitude of the dithering signal.

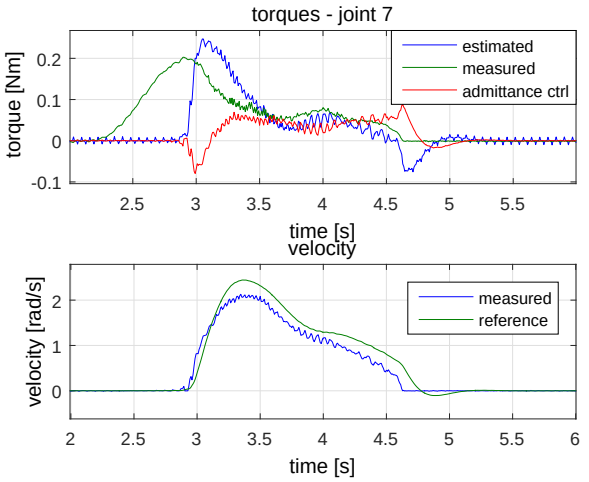

Fig. 5. The contribution of the admittance control in active LTP is illustrated. The controller contributes by smoothing out and helping the movement according to the defined mass and damping properties. Note that the reference velocity is overall slightly higher than the measured one.

B. Active Lead-through Programming

Several experiments were done to explore the combination of feedforward and admittance control described in Sec. II-A. We could tune the matrices $\tilde{M}$ and $\tilde{D}$ in real-time on the external research interface [15] to modify the response of force control. However, to avoid possible instabilities, the desired inertia matrix was chosen higher than half of the mechanical one. Generally, the feedforward compensation of friction is applied earlier than the force feedback because of the time needed by the observer to converge to the external forces.

In the experiment presented in Fig. 5, a damping matrix $\tilde{D}$ with small values was set, in order to facilitate the handling of the robot. It can be seen that the admittance control torque (red line) contributes by smoothing out the movement in the beginning and the end of the movement and helping the rotation in the middle. Thus, the motor actively favors the rotation of the joint. Since this experiment concerns the wrist joint of the robot (where the tool is mounted), the order of magnitude of the torques is extremely small, and for this reason the uncertainties in the friction model and the resulting error in torque estimation are emphasized.

C. Comparison with a Passive LTP

The active lead-through programming implemented in this paper was compared to a passive LTP system, in order to obtain a qualitative idea of the improvements achieved with the active version. We used the passive LTP implemented in the Robotics Lab of Lund University as the benchmark. More details can be found in [8], [11] and [17].

In this test, a joint of YuMi was rotated manually and the applied force was measured by a force sensor mounted on the end-effector. The test was repeated twice, once using the active LTP and the other time using the passive implementation. The data of the two different experiments

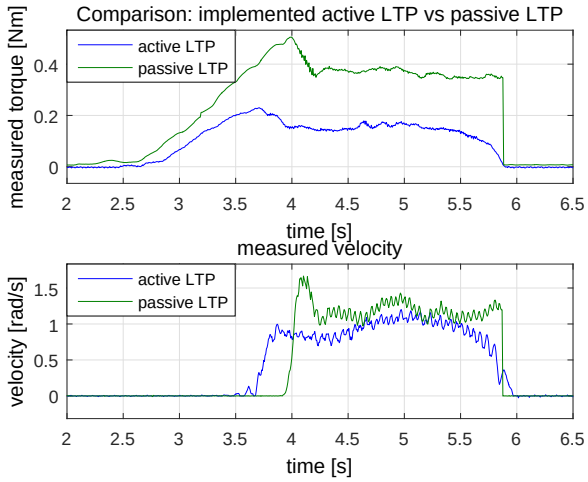

Fig. 6. Comparison between a passive LTP previously implemented on YuMi [8] and the active LTP. Using the two different implementations, the external forces (measured with a force sensor) were compared for generating a similar movement of a joint. The external torque required for the active LTP is almost half of the passive solution and the joint starts rotating earlier.

have been overlapped in Fig. 6. Since the external torque was applied by hand, the resulting displacement and velocity are not identical in these two experiments. However, as it can be seen in the lower graph in Fig. 6, the resulting velocities are very similar, hence a similar value of the friction in the joint during the rotation can be assumed. In this comparison, the required external torque for rotating the joint in the passive LTP is almost twice as much as the active implementation. The onset of motion is also earlier despite a lower level of external forces in the active implementation.

IV. Discussion

An active lead-through programming system implemented by an admittance control based on the estimated external torques has been presented. The combination of admittance

control and feedforward friction compensation has proven useful, specially as soon as the joints start moving. The feedforward torque immediately affects the system. Therefore, it reduces the nonlinearity of the system and contributes to its stability. The resulting control torque makes the robot easier to handle and smoother in the movements. The combination shows a stable behavior in stiff contact situations (watch the submitted video). In this paper, we did not address the step from a demonstration to a program, and analysis of the stability ensuring the passivity of the components is our future research.

Since no measurements of external torque are available, the estimate of the external torques using the Kalman filter is based on the model of the manipulator. This means that the quality of the estimated torque depends on the model of the robot, in particular on the friction model. Therefore, an accurate friction model and a gravity model are crucial.

The feedforward dithering torque applied at almost-zero velocity drastically reduces the required initial force to overcome the static friction. As a result, the motion starts with a lower force and at the same time the performance of the observer improves remarkably. Dithering mitigates the intrinsic limitation of detecting external forces by the model-based Kalman filter when the joint is not moving.

For modeling external forces (12), a better assumption than constant forces at the joint space would be constant forces at the operational space. The corresponding A_τ can be derived by differentiating (20) w.r.t. time. However, this result in a state-dependent matrix that requires solving the more complex state-dependent differential Riccati equation [18].

The force control allows modifying the behavior of the robot in multiple scenarios and makes it possible to introduce virtual constraints during the lead-through programming. In comparison with the passive LTP previously implemented on the same robot [8], our approach shows improvements in terms of ease of handling and flexibility. This can be observed as lower force required to move the joints and quicker onset of movements.

V. Conclusion

In this paper, an active sensorless lead-through programming algorithm, i.e., with a force-feedback control loop and without any force sensors was presented. The control architecture consists of an admittance control as well as a force observer. The force observer provides an estimation of the external torques, which in turn is the input to the admittance control. The observer is a Kalman filter based on the generalized momentum formulation, which is free from matrix inversion and any numerical differentiation.

Although approaches based on the generalized momentum formulation suffer from the inability to detect forces at zero velocity, we showed applying a dithering torque at high frequency can largely mitigate this problem. This is possible by practically reducing the static friction in the motor side of the gear box and putting the robot always on the onset of the movement.

Our active lead-through algorithm fulfills the expectations in terms of smoothness and ease of handling, maintaining stability in critical situations when the arm hits stiff surfaces or becomes constrained during contact. The advantages of an active LTP are multiple. In comparison with the passive approach [8], the interaction forces are reduced almost by half. Furthermore, it gives the possibility to modify the behavior of a manipulator depending on the teaching scenario.

References

[1] P. Hacksel and S. Salcudean, "Estimation of environment forces and rigid-body velocities using observers," in *Proc. IEEE Int. Conf. Robotics and Automation (ICRA), May 8-13, San Diego, CA*, pp. 931–936, 1994.

[2] A. Alcocer, A. Robertsson, A. Valera, and R. Johansson, "Force estimation and control in robot manipulators," in *Proc. 7th IFAC Symp Robot Control 2003 (SYROCO'03), Sep. 1-3, Wrocław, Poland*, vol. 1, p. 55, 2004.

[3] A. De Luca and R. Mattone, "Sensorless robot collision detection and hybrid force/motion control," in *Proc. IEEE Int. Conf. Robotics and Automation (ICRA), Apr. 18-22, Barcelona, Spain*, pp. 999–1004, 2005.

[4] T. Murakami, F. Yu, and K. Ohnishi, "Torque sensorless control in multidegree-of-freedom manipulator," *IEEE Tran. Ind. Elec.*, vol. 40, no. 2, pp. 259–265, 1993.

[5] M. Van Damme, P. Beyl, B. Vanderborght, V. Grosu, R. Van Ham, I. Vanderniepen, A. Matthys, and D. Lefeber, "Estimating robot end-effector force from noisy actuator torque measurements," in *Proc. IEEE Int. Conf. Robotics and Automation (ICRA), 9-11 May, Shanghai, China*, pp. 1108–1113, 2011.

[6] A. Wahrburg, E. Morara, G. Cesari, B. Matthias, and H. Ding, "Cartesian contact force estimation for robotic manipulators using kalman filters and the generalized momentum," in *Proc. IEEE Int. Conf. Automation Science and Engineering (CASE), Aug. 24-28, Gothenburg, Sweden*, pp. 1230–1235, 2015.

[7] M. Ragaglia, A. M. Zanchettin, L. Bascetta, and P. Rocco, "Accurate sensorless lead-through programming for lightweight robots in structured environments," *Robotics and Computer Integrated Manufacturing*, vol. 39, pp. 9–21, June 2016.

[8] A. Stolt, F. B. Carlson, M. Ardakani, I. Lundberg, A. Robertsson, and R. Johansson, "Sensorless friction-compensated passive lead-through programming for industrial robots," in *Proc. IEEE/RSJ Int. Conf. Intelligent Robots and Systems (IROS), Sep. 28-Oct. 2, Hamburg, Germany*, pp. 3530–3537, 2015.

[9] A. Stolt, A. Robertsson, and R. Johansson, "Robotic force estimation using dithering to decrease the low velocity friction uncertainties," in *Proc. IEEE Int. Conf. Robotics and Automation (ICRA), May 26-30, Seattle, Washington*, (Seattle, WA, USA), pp. 3896–3902, 2015.

[10] B. Siciliano and O. Khatib, eds., *The Handbook of Robotics*, ch. 7, pp. 164–170. Berlin Heidelberg: Springer, 2008.

[11] A. Stolt, *On Robotic Assembly using Contact Force Control and Estimation*. PhD Thesis, Dept. Automatic Control, Lund University, Lund, Sweden, Sep 2015. TFRT--1109--SE.

[12] B. Siciliano, L. Sciavicco, L. Villani, and G. Oriolo, *Robotics. Modelling, Planning and Control*, pp. 161–189. Springer Verlag, 2009.

[13] H. Kwakernaak and R. Sivan, *Linear optimal control systems*, vol. 1. Wiley-interscience, New York, 1972.

[14] ABB Robotics, "YuMi product page." `http://new.abb.com/products/robotics/yumi`. Accessed: 2015-01-15.

[15] A. Blomdell, I. Dressler, K. Nilsson, and A. Robertsson, "Flexible application development and high-performance motion control based on external sensing and reconfiguration of ABB industrial robot controllers," in *Proc. ICRA 2010 Workshop on Innovative Robot Control Architectures for Demanding (Research) Applications*, (Anchorage, Alaska), pp. 62–66, May 2010.

[16] ATI, "Force/Torque transducers." `http://www.ati-ia.com/products/ft/sensors.aspx`. Accessed: 2015-12-22.

[17] M. M. Ghazaei Ardakani, "Topics in trajectory generation for robots," Licentiate Thesis TFRT--3265--SE, Dept. Automatic Control, Lund University, Sweden, 2015.

[18] D. A. Haessig and B. Friedland, "State dependent differential riccati equation for nonlinear estimation and control," in *Proc. 15th IFAC Triennial World Congress, 21-26 Jul., Barcelona, Spain*, 2002.